Atmos. Chem. Phys. Discuss., 11, 19357–19393, 2011
www.atmos-chem-phys-discuss.net/11/19357/2011/
doi:10.5194/acpd-11-19357-2011

Atmospheric Chemistry and Physics Discussions

Impacts of 2006 Indonesian fires on tropical upper tropospheric carbon monoxide and ozone

L. Zhang[1], Q. Li[1], J. Jin[2], H. Liu[3], N. Livesey[2], J. Jiang[2], Y. Mao[1], D. Chen[1], and M. Luo[2]

[1]Department of Atmospheric and Oceanic Sciences, University of California, Los Angeles, CA, USA
[2]Jet Propulsion Laboratory, California Institute of Technology, Pasadena, CA, USA
[3]National Institute of Aerospace, Hampton, VA, USA

Received: 17 June 2011 – Accepted: 29 June 2011 – Published: 6 July 2011

Correspondence to: Q. Li (qli@atmos.ucla.edu)

Published by Copernicus Publications on behalf of the European Geosciences Union.

Abstract

We investigate the relative impacts of biomass burning emissions and dynamics on tropical upper tropospheric carbon monoxide (CO) and ozone (O_3) over western and central Indonesia during the August-November 2006 fires in equatorial Asia by using a global three-dimensional model of tropospheric chemistry (GEOS-Chem) and by comparing model results with Microwave Limb Sounder (MLS) observations of upper tropospheric CO and O_3. GEOS-Chem CO and O_3 reproduce MLS observed enhancements from convective lifting of fire emissions. In the tropical upper troposphere (UT), fire effluents from equatorial Asia are primarily transported southwestward to the eastern tropical Indian Ocean, driven by the high-pressure systems along 10° N–15° N and 10° S–15° S latitudes, and northeastward to southeast Asia and beyond, driven by the western North Pacific subtropical high. A characteristic feature of these CO enhancements is that they lag behind biomass burning emissions (by 2–3 weeks) at the three pressure levels from 215 hPa to 100 hPa, resulting form the decreasing influence of deep convective lifting with altitude in the UT. We estimate the fire influences by contrasting one model simulation with year-specific and another with climatological biomass burning emissions. Biomass burning accounts for about 50–150 ppbv of CO and 5–20 ppbv of O_3 in the tropical UT below 100 hPa during October and November, with temporal variations driven by biomass burning and deep convection. We estimate the dynamic impacts by examining the difference between a model simulation for 2006 (El Niño) and another for 2005 (neutral). The dynamic impacts are far more complex and account for up to 100 ppb of CO and 30 ppb of O_3 in the tropical UT below 100 hPa. The temporal variation of the dynamic impact on CO is driven by deep convection. The variation of the dynamic impact on O_3 not only depends on deep convection but also reflects the non-linearity of O_3 chemistry.

ACPD
11, 19357–19393, 2011

1 Introduction

Smoke and excess tropospheric ozone from biomass burning have long been observed over the tropics (Thompson et al., 2001). In equatorial Asia, droughts during El Niño events are typically followed by large fires (van der Werf et al., 2008a). Previous modeling studies have shown that dynamic processes related to El Niño events and the shift in the large-scale Walker circulation also contributed to the observed enhancements in tropospheric O_3 columns over the equatorial Western Pacific during Indonesian fire seasons (Sudo and Takahashi, 2001; Chandra et al., 2002, 2004; Doherty et al., 2006). The fire emissions and the perturbed dynamics together result in variations in tropospheric composition (Chandra et al., 2002; Ziemke and Chandra, 2003). Doherty et al. (2006) showed that tropospheric ozone column over equatorial Asia and west Pacific was modulated by the El Niño-Southern Oscillation (ENSO). On the other hand, aerosols produced by these fires had strong influence on tropical atmospheric dynamics (Ott et al., 2010). There was a possible positive feedback in which the anthropogenic burning in Indonesia enhanced drought stress during El Niño (Tosca et al., 2010).

These large fires significantly alter tropospheric composition including aerosol loading and tropospheric ozone and CO (Duncan et al., 2003a). Duncan et al. (2007) used the Global Modeling Initiative (GMI) chemical transport model (CTM) to estimate that these fires increased CO by more than 40 % in the tropical tropopause layer and by more than 10 % in the lower stratosphere for several months. Their results also demonstrated that the increased presence of CO from the Indonesian fires could reduce OH levels thereby increasing the atmospheric lifetimes and troposphere-to-stratosphere transport of trace gases. Chandra et al. (2002) studied the effects of forest fires in the Indonesian region during the 1997 El Niño and found that about half of the increase in tropospheric column ozone was due to biomass burning and the other half was due to dynamical effects. Logan et al. (2008) examined observations from the Tropospheric Emissions Spectrometer (TES) to study the influences of the 2004 and

ACPD
11, 19357–19393, 2011

2006 El Niño events on tropical tropospheric profiles of CO, O_3 and water vapor. Their results showed that 511 hPa CO and O_3 mixing ratios were on average 80 ppbv and 15–30 ppbv larger in October and November of 2006 than in the corresponding months of 2005 over the Indonesian region. In the region of highest CO (200 ppb), the contribution of the fires to enhanced O_3 was 45 % in October, 75 % in early November, and 10 % in December. Dynamical changes increase O_3 over a larger region than fire emissions which mainly increase O_3 at 10° N–10° S in October and November. Ziemke et al. (2009) used satellite observations and the GMI model to estimate that fire emissions led to increases of tropospheric ozone mixing ratios in the Indonesian region by 15–25 % during the 2006 Indonesian fires. Chandra et al. (2009) used the GMI model to separate the dynamical impact of the 2006 El Niño from changes in fire emissions. They found that emissions and dynamical changes contributed almost equally to observed ozone increases over Indonesia in October and November, though changes because of emissions were centered in the Indonesian region while dynamical changes were over the Indian and western Pacific Oceans. The global burden of CO increased by 8–12 % from October through December as a result of the 2006 fires (Chandra et al., 2009).

The emissions from the 2006 equatorial Asia fires were larger than any other years during 1997–2007 except 1997 (van der Werf et al., 2006, 2008a). Various satellite observations have shown enhanced CO levels throughout the troposphere during these fires (Logan et al., 2008; Rinsland et al., 2008; Chandra et al., 2009; Nassar et al., 2009). Many previous studies of the Indonesian fires, including the ones in 2006, have focused largely on the lower and middle tropospheric CO, O_3 and aerosols and on tropospheric ozone columns. In this study, we analyze Microwave Limb Sounder (MLS) measurements of CO and O_3 to investigate the impact of the 2006 Indonesian fires on the tropical upper tropospheric CO and O_3 over equatorial Asia. Our approach is to apply a global three-dimensional chemical transport model to interpret the MLS observations. We intend to delineate the relative importance of the fire emissions and the dynamics in influencing the tropical UT CO and O_3 over equatorial Asia. We give a

ACPD
11, 19357–19393, 2011

brief description of the 2006 Indonesian fires during August-November 2006 in Sect. 2. Section 3 presents MLS observations of upper tropospheric CO, O_3 and cloud ice water content (IWC). Model simulations of tropical UT CO and O_3 during the fires are discussed in Sect. 4. The relative impacts of biomass burning and dynamics on the UT CO and O_3 are examined in Sect. 5. A summary and conclusions are presented in Sect. 6.

2 The 2006 Indonesian fires

Climate strongly regulates fire emissions and deforestation in equatorial Asia (van der Werf et al., 2008a, b). Previous studies have shown that fire emissions in equatorial Asia show strong interannual variability and increase significantly during El Niño (Bowen et al., 2001; Heil and Goldammer, 2001; van der Werf et al., 2006). The extended dry season during El Niño periods enables more effective use of fires for land management purpose, which often leads to widespread fires (van der Werf et al., 2008b). Fires in Indonesia were intentionally set to clear out cropland and for industrial expansion during the dry season of El Niño. Some of these fires got out of control and led to extensive burning, for instance in 1997 (Duncan et al., 2003 and references therein) and 2006 (ver der Werf et al., 2008). During the 2006 moderate El Niño, large and widespread fires occurred in Indonesia, Malaysia, and northern Australia during the extended dry season (August through November) (van der Werf et al., 2008a, b). Figure 1a shows the total CO emissions from August to November 2006 with largest emissions in southern Borneo, Sumatra, and northern Australia. The emission data are from the Global Fire Emissions Database (GFED v2) (van der Werf et al., 2006). Much of our analysis focuses on western and central Indonesia (EQ-10° S latitudes, 100–125° E longitudes), referred to hereafter as the WCI domain (the blue rectangle in Fig. 1a). Figure 1b shows the monthly CO emissions for the WCI domain from 1997 to 2008. Large emissions occurred during the 1997, 2002, 2004, and 2006 El Niño. Emissions from Borneo during the 2006 were more than 30 times higher than

ACPD
11, 19357–19393, 2011

emissions during the 2000 La Niña (van der Werf et al., 2008). The 2006 fires started in August and lasted through late November (Fig. 1c). Peak emissions of CO were seen in both early October and from late October to early November. There was a broad peak for much of August and early September. The CO emissions in October 2006 were several hundred times larger than the climatological values for this region.

3 MLS observations of upper tropospheric O_3 and CO

The Microwave Limb Sounder (MLS) instrument (Waters et al., 2006) aboard the Aura spacecraft has been measuring atmospheric parameters since August 2004 (Schoeberl and Talabac, 2006). MLS uses microwave limb sounding to measure temperature and chemical constituents, including CO, water vapor, O_3 and cloud ice water content (IWC) in the UT (pressure $\leq$215 hPa) and stratosphere with a vertical resolution of ~4.5 km and a horizontal resolution of ~3° along the orbit (Livesey et al., 2006). MLS chemical composition measurements in the UT are generally not degraded by the presence of clouds because the typical cloud particle sizes are much smaller than the wavelength of the radiation being observed. The CO, O_3 and cloud IWC observations used here are MLS retrieval version 3.3 (Livesey et al. 2011). The observations are averaged onto 2° latitude ×5° longitude grids for every five days. Our analysis focuses on the observations for pressure levels 100 hPa, 147 hPa, and 215 hPa. Previous (version 2) biases of MLS upper tropospheric CO at 215 hPa and partly at 146 hPa have been ameliorated in version 3.3 compared with previous versions (Livesey et al., 2011).

MLS cloud IWC was derived from the 240-GHz cloud-induced radiances at high tangent heights and is scientifically useful at 215–83 hPa (Wu et al. 2008). We include the IWC data in our analysis because it is a proxy for deep convection in the UT (Fu et al., 2006; Jiang et al., 2010; Jiang et al., 2011): larger IWC indicates stronger deep convection. In addition to MLS cloud IWC data, we also examined NOAA outgoing longwave radiation (OLR) interpolated from satellite observations (Liebmann and Smith, 1996). OLR is a widely used proxy for deep convection with lower values indicating stronger

ACPD
11, 19357–19393, 2011

deep convection (Randel et al., 2006; Logan et al., 2008; Nassar et al., 2009). The OLR data are global, daily data with a horizontal resolution of 2.5°×2.5°. We averaged the OLR data for every five days as we did for MLS data. The year 2005 was a neutral year from El Niño perspective. As in Chandra et al. (2007, 2009) and Logan et al. (2008), we choose August–November of 2005 as baseline for estimating El- Niño-related changes in these months in 2006. Here we compared the IWC and OLR data between 2006 and 2005 to get a better understanding of the different deep convection activities over equatorial Asia between these two years. Figure 2 shows the differences of IWC at 147 hPa and 215 hPa, and OLR between 2006 and 2005, calculated as 2006 values minus those of 2005, from July to December over the WCI domain. Both the IWC and OLR data show that deep convective activities over the WCI domain from October to middle December were considerably weaker in 2006 than in 2005.

Figure 3 shows MLS CO concentrations (5-day averages) in the tropical UT at 215 hPa, 147 hPa, and 100 hPa for 2005 and 2006. Again, we included 2005 here for comparison because it was a neutral year and the fire emissions over the Indonesia domain were considerably smaller than those from 2006 (Fig. 1b). Strongly enhanced CO concentrations are clearly evident from August to November 2006 at all three pressure levels with maximum CO concentrations exceeding 150 ppb at 215 hPa and 147 hPa and 110 ppb at 100 hPa. At 147 hPa and 215 hPa, the year-over-year enhancements during October–November are more than 70 % from 2005 to 2006. The enhancements are widespread between 20° S and 10° N latitudes. Some noticeable time lags are seen in the CO enhancements among the pressure levels – the enhancements at 100 hPa lag those at 147 hPa and the latter lag behind those at 215 hPa. These time lags likely reflect the gradual upward propagation (via advection) of the convectively lofted surface biomass burning emissions (Liu et al., 2010). Correspondingly, the CO concentrations from the Tropospheric Emission Spectrometer (TES) retrievals also showed a very strong maximum over Indonesia and the Indian Ocean with peak concentrations exceeding 200 ppb in October and November in the lower troposphere (825–511 hPa) (Logan et al., 2008; Nassar et al., 2009). In addition, both very high CO concentrations

ACPD
11, 19357–19393, 2011

in the middle to UT (400–200 hPa) observed by the Atmospheric Chemistry Fourier Transform Spectrometer (ACE-FTS) (Rinsland et al., 2008) and high CO columns by the Measurement Of Pollution In The Troposphere (MOPITT) instrument (Yurganov et al., 2008) were also seen over the same broad region during the 2006 Indonesian fires. These observations clearly showed that the biomass burning emissions from the large fires of 2006 over Indonesia significantly enhanced the CO concentrations in the middle to UT over that region. The biomass burning emissions from northern Australia (Fig. 1a) likely also contributed to these enhancements. We will address the Australia fire contribution in subsequent sections.

Figure 4 shows the time-latitude cross-sections of MLS O_3 (5-day averages) at 215 hPa, 147 hPa, and 100 hPa for 2005 and 2006. Significant enhancements in O_3 are clearly seen at 147 hPa and to a lesser degree at 215 hPa in October and November 2006 relative to 2005. Ozone enhancements at 100 hPa due to the Indonesian fires, if any, are difficult to quantify because of the already high background O_3 concentrations near the tropical tropopause. The enhancements at 215 hPa are mainly confined to south of the equator with increases of 15–20 ppb during October and November 2006 relative to 2005. It is probable that these enhancements were influenced by the emissions from the 2006 Indonesian fires. We will address that in the following sections.

4 GEOS-Chem model description and simulations

GEOS-Chem is a global three-dimensional chemical transport model (Bey et al., 2001) driven by assimilated meteorological observations from the Goddard Earth Observing System (GEOS) of the NASA Global Modeling and Assimilation Office (GMAO). We use GEOS-Chem version 8-01-04 (http://acmg.seas.harvard.edu/geos/) driven by GEOS-4 and GEOS-5 meteorological fields with 6-h temporal resolution (3-h for surface variables and mixing depths), 2° (latitude) × 2.5° (longitude) horizontal resolution, and 30 (GEOS-4) or 47 (GEOS-5) vertical layers between the surface and 0.01 hPa. The GEOS-Chem model includes a detailed description of tropospheric O_3-

ACPD
11, 19357–19393, 2011

NO_x-hydrocarbon chemistry coupled with aerosol chemistry (Bey et al., 2001). Gas phase chemical reaction rates and photolysis cross sections are taken from Sander et al. (2000). Photolysis frequencies are computed using the Fast-J algorithm (Wild et al., 2000).

Tracer advection is computed every 15 min with a flux-form semi-Lagrangian method (Lin and Rood, 1996). Tracer moist convection is computed using the GEOS convective, entrainment, and detrainment mass fluxes as described by Allen et al. (1996a, b). The deep convection scheme of GEOS-4 is based on Zhang and McFarlane (1995), and the shallow convection treatment follows Hack (1994). GEOS-5 convection is parameterized using the relaxed Arakawa-Schubert scheme (Moorthi and Suarez, 1992). ^{222}Rn is commonly used as a tracer for diagnosing convection in chemical transport model (Jacob and Prather, 1990; Considine et al., 2005). Figure 5 compares the annual zonal mean distributions of ^{222}Rn for 2004 simulated by GEOS-Chem driven by GEOS-4 and GEOS-5, respectively. The tropical upper tropospheric ^{222}Rn concentrations are much higher in the model results from the simulation driven by GEOS-4 meteorological data than those from the simulation driven by GEOS-5 data. These differences indicate that the deep convection in the tropics, especially in the northern tropics, is significantly deeper in GEOS-4 than in GEOS-5 (Liu et al., 2010). GEOS-Chem simulations of the tropical upper tropospheric CO and O_3 will undoubtedly bear these differences, as discussed in subsequent sections.

The fossil fuel emissions are from the Emission Database for Global Atmospheric Research (EDGAR) inventory for NO_x, CO, and SO_2 (Olivier et al., 2001) and from the Global Emission Inventory Activity (GEIA) for other chemical compounds (Benkovitz et al., 1996) with additional updates as described by Hudman et al. (2007). Asian anthropogenic emissions are updated with the estimates from Zhang et al. (2009). Biofuel emissions are from Yevich and Logan (2003). The biogenic VOCs emissions are based on the Model of Emissions of Gases and Aerosols from Nature (MEGAN) inventory (Guenther et al., 2006). The lightning NO_x emissions are parameterized based on cloud top height and regionally scaled to climatological satellite observations

ACPD
11, 19357–19393, 2011

of flash rates (Hudman et al., 2007; Sauvage et al., 2007).

Biomass burning emissions are from the Global Fire Emission Database version 2 (GFEDv2) that resolves the interannual variability of biomass burning emissions (van der Werf et al., 2006; Randerson et al., 2006). GFEDv2 was derived using satellite observations including active fire counts and burned areas in conjunction with a biogeochemical model. Carbon emissions were calculated as the product of burned area, fuel loads and combustion completeness. Burned area was derived using active fire and 500-m burned area datasets from the Moderate Resolution Imaging Spectroradiometer (MODIS) as described by Giglio et al. (2006). The original GFEDv2 inventory has a spatial resolution of 1° (latitude) ×1° (longitude) and a monthly temporal resolution. The emissions were re-sampled to 2° (latitude) ×2.5° (longitude) grids for use in our GEOS-Chem simulations. Forest fires typically last from several days to weeks as seen in MODIS active fires (Giglio et al., 2003). Therefore, the monthly GFEDv2 emissions were re-sampled to an 8-day time step according to MODIS 8-day active fire counts (Chen et al., 2009). The 8-day GFEDv2 emissions were used for the model simulations presented here unless stated otherwise. Additionally, a climatological monthly mean biomass burning emission inventory from Duncan et al. (2003a) is also included in the model and were used in two simulations.

We conducted several model simulations for 2006 and 2005 driven by either GEOS-4 or GEOS-5 meteorological data. Either 8-day GFEDv2 or climatological biomass burning emissions were used in these simulations. Justifications for these simulations are provided where appropriate. The details for these experiments are summarized in Table 1. For direct comparison with MLS observations, we extracted model results at the time and location of the observations and applied the same 5-day averaging as we did for the observations (see Sect. 2).

Our standard simulation (experiment A) is driven by GEOS-4 meteorological data and with 8-day GFEDv2 emissions for 2006. Figure 6 compares model simulated and MLS retrieved CO concentrations at 100 hPa, 147 hPa, and 215 hPa for 2006 over equatorial Asia and northern Australia between 20° S and 20° N. The values shown

ACPD
11, 19357–19393, 2011

are averages between 100° E and 125° E longitudes. GEOS-Chem CO reproduces the seasonal cycles seen in MLS data at all three pressure levels: broad enhancements in spring (March), relatively low concentrations in summer (June–July), and large extensive enhancements in October–November. In addition, model CO also captures the time lags in the October–November enhancements among the three pressure levels: the enhancements extend to well in December at 147 hPa and 100 hPa. Model CO concentrations are generally lower than MLS data at all three pressure levels with largest differences of more than 50 ppbv at 100 hPa during the peak fire season in October and November. Part of these discrepancies is due to the weak convection in the model hence insufficient convective lofting of surface biomass burning emissions to the tropical UT over equatorial Asia. Nassar et al. (2009) compared GEOS-4 OLR with NOAA interpolated OLR for October and November 2006 and concluded that GEOS-4 convection was too weak over equatorial Asia in Java, Borneo, and New Guinea. Additionally, part of the discrepancies is explained by the positive biases in MLS CO at these pressure levels despite significant bias reductions in MLS v3.3 data (Livesey et al., 2006, 2011). Previous studies have shown that outflow of CO from East Asia were transported in the UT to tropical South and Southeast Asia (Liu et al., 2003; Li et al., 2005). The lower concentrations simulated by the model at the northern edge of the domain thus likely reflect in part the insufficient transport of CO from East (and Southeast) Asia in the model.

Figure 7 shows the model simulated and MLS observed spatial distributions of monthly averaged CO concentrations at 215 hPa in October and November 2006. Also shown are streamlines from the NCEP/NCAR reanalysis data. Significant enhancements of CO concentrations are seen over equatorial Asia in both the model results and the observations. The spatial extents of the enhancements are larger in the observations than in the model results, especially in November. Sandwiched by the high-pressure systems along 10° N–15° N and 10° S–15° S latitudes, the outflow of biomass burning CO in both months is mainly to the Eastern tropical Indian Ocean in both hemispheres. Northeastward outflow to Southeast Asia under the influence of the western

ACPD
11, 19357–19393, 2011

North Pacific subtropical high, both in the observations and in the model, is also evident. We find similar CO outflow patterns at 147 hPa (not shown).

Figure 8 shows GEOS-Chem simulated and MLS observed O_3 at 215 hPa and 147 hPa for 2006. Values are averages over the 100–125° E longitudes. At 215 hPa, the highest O_3 levels during October–December are seen over the southern tropics extending from the equator to 20° S in both the observations and the model results. The observed high O_3 concentrations in May are less obvious in the model results. These high O_3 concentrations in May appear to be a recurring feature and are related to lightning NO_x emissions (Zhang et al., Lightning impact on tropical upper tropospheric ozone over tropical southern Indian Ocean, manuscript in preparation). The observations show high O_3 concentrations at 147 hPa during late October–November while the model results show correspondingly considerably lower values. The 100 hPa pressure level is either at or close to the tropical tropopause where the already high O_3 concentrations make it challenging to detect O_3 enhancements, if any, due to convectively lifted biomass burning emissions.

It is conceivable that biomass burning emissions in northern Australia during October and November 2006 (Fig. 1a) may contribute to the upper tropospheric CO over equatorial Asia. Luo et al. (2009) examined satellite observations of CO during December 11-19, 2006 from MLS and the Tropospheric Emission Spectrometer (TES) (Beer et al., 2006) downwind of the Australian fires. They found significant amount of northern Australia biomass burning emissions lifted to the middle and UT. To quantify the influence of northern Australia fire emissions on tropical upper tropospheric CO and O_3, we conducted a GEOS-Chem sensitivity simulation where biomass burning emissions in Australia (110°–179° E, 11°–50° S) were shut off. The differences with the standard simulation (experiment A) thus represent the impact of Australia biomass burning emissions for October and November 2006. The results show that northern Australia biomass burning has rather small influences on the tropical upper tropospheric CO (less than 10 ppbv or 6 % of the total CO) and O_3 (less than 4 ppbv or 4 % of the total O_3).

ACPD
11, 19357–19393, 2011

Figure 9 show MLS observed and model simulated CO at 100 hPa, 147 hPa, and 215 hPa and O_3 at 147 hPa and 215 hPa over the WCI domain from July to December 2006. Also shown are MLS cloud IWC at 215 hPa and GFEDv2 CO emissions. The maximum MLS CO concentrations are seen in late October with more than 300 ppbv at 215 hPa, 250 ppbv at 147 hPa, and 120 ppbv at 100 hPa. The second peaks are seen in early November at 215 hPa and 147 hPa. It is more than twice increase compared with the background CO concentrations (Fig. 9a). The MLS CO concentrations started to increase in the early October at 215 hPa and 147 hPa, about 2–3 weeks after the onset of the biomass burning. The cloud IWC increased at the same time as the enhancements of MLS CO. The increased convection might possibly contribute to the increase of CO concentrations after the large biomass burning. Both the MLS CO concentration and biomass burning emissions showed two peaks with the same time lag. The largest CO enhancement is therefore a combined effect of both relative stronger convection and large biomass burning emission from Indonesian fires. GEOS-Chem CO shows an extended maximum of CO concentrations (up to 300 ppbv) at 215 hPa from October to November, in broad agreement with the MLS observations (Fig. 9b). Model CO at 147 hPa shows elevated concentrations (~150 ppbv) during the second half of October. The peak concentrations at 147 hPa are much lower in the model results than in the observations. Part of the difference is again attributable to the weak deep convection in GEOS-4 during October and November 2006. The observed November enhancements at 147 hPa are entirely absent in the model results.

The MLS O_3 concentrations also show similar double peaks at 147 hPa and, to a lesser extent, 215 hPa in October and November 2006, respectively (Fig. 9c). GEOS-Chem O_3 shows enhanced concentrations at both 215 hPa and 147 hPa in September and October 2006 (Fig. 9d). The simulated concentrations are much lower than the observations.

ACPD
11, 19357–19393, 2011

5 Impact of biomass burning and dynamics on upper tropospheric O_3 and CO

The distribution of UT pollutants, such as O_3 and CO, can be influenced both by surface emission sources and by dynamical factors, such as convection and horizontal winds (e.g. Jiang et al., 2007). Chandra et al. (2007, 2009) have shown that both biomass burning and meteorological changes contributed almost equally to the observed increases in tropospheric column O_3 over Indonesia during the dry seasons of the 1997 and the 2006 El Niño. We investigate here the relative influence of the 2006 Indonesian biomass burning and dynamics on the tropical upper tropospheric CO and O_3 over equatorial Asia. For this purpose we conducted two GEOS-Chem sensitivity simulations as summarized in Table 1. We first conducted a model simulation driven by GEOS-4 meteorological data for 2006 (experiment A1) where a monthly mean climatological biomass burning emissions from Duncan et al. (2003a) were used in lieu of the 8-day GFEDv2 inventory for 2006 as used in experiment A, the standard simulation. Experiments A1 and A share the same configuration except for the aforementioned different biomass burning emission inventories used. The differences between the results from these two simulations, presented in Fig. 10 for the WCI domain, thus show the impact of enhanced biomass burning emissions. We then conducted a simulation driven by GEOS-4 meteorological data for 2005 (experiment A2) with otherwise the same configuration as the standard simulation. The differences between these two experiment results, shown in Fig. 11 for the WCI domain, therefore reflect the differences in the dynamics between the 2006 El Niño and 2005, a neutral year from an El Niño perspective. We discuss these differences as shown in Figs. 10 and 11 in more detail later in this section.

It is conceivable that the deep convection parameterizations used in the GEOS reanalysis system and the GEOS-Chem model strongly influence the abovementioned impacts. To examine this sensitivity, we conducted three GEOS-Chem simulations driven by GEOS-5 meteorological data (experiments B, B1, and B2), which differs significantly from GEOS-4 data in the deep convection scheme used (Sect. 4). Other than

ACPD
11, 19357–19393, 2011

the GEOS-5 meteorological data used, experiments B, B1, and B2 mirror experiments A, A1, and A2, respectively. We can then examine the impacts of the 2006 Indonesian biomass burning emissions and dynamics with experiments B, B1, and B2 exactly as we do with experiments A, A1, and A2. The results are also shown in Figs. 10 and 11.

At 215 hPa, the biomass burning emissions contribute about 60–120 ppbv (GEOS-5) to 80–180 ppbv (GEOS-4), depending on the meteorological data used to drive the model simulations, to the CO enhancements during much of October and November 2006 (Fig. 10a). The CO enhancements show secondary peaks during early to middle September. The model results thus show a persistent biomass burning impact on the upper tropospheric CO concentrations during the 2006 Indonesian fire season. The stronger deep convection in GEOS-4 than in GEOS-5 largely explains the dependence of the model results on the meteorological data used. Figure 12 compares the convective precipitation and cloud top height, both proxies for deep convection, from GEOS-4 and from GEOS-5 during July–December 2006 averaged over the WCI domain. The convective precipitation is consistently larger and the cloud top is higher in GOES-4 than in GEOS-5 through much of the period. The temporal variation of convective precipitation is also markedly different between GEOS-4 and GEOS-5.

The influences from dynamics are more complex. The corresponding influences at 215 hPa from dynamics (Fig. 10b) amount to about 30–50 ppbv (GEOS-5) to 70–120 ppbv (GEOS-4) of the CO enhancements during much of October 2006. In comparison, the biomass burning influences at 215 hPa are not only larger but also more extensive throughout October and November 2006. Results from the simulation driven by GEOS-4 meteorological data show sharp decreases hence relatively small influence (less than 10 ppb CO) from dynamics during November 2006. In contrast, results from the simulation driven by GEOS-5 meteorological data show decreases of up to 40 ppb CO during late October and early November 2006 and CO enhancements of about 50 ppb during middle November 2006. Clearly both the magnitudes and the temporal variations of the biomass burning and the dynamic impacts differ between the two model simulations. These differences are mostly because of the differing strengths and

ACPD
11, 19357–19393, 2011

temporal variations of the deep convection in GEOS-4 and GEOS-5 (Fig. 12).

At 147 hPa, the biomass burning emissions contribute about 40–70 ppbv to the CO enhancements during middle to late October 2006 (Fig. 10a). The biomass burning influences for October 2006 are comparable between the two model simulations. The differences are in November when results from the simulation driven by GEOS-4 meteorological data decrease sharply through November while results from the simulation driven by GEOS-5 meteorological data show another maxima of 40–60 ppb of CO. Again, these differences are because of the different temporal variations of deep convection during October and November 2006 in GEOS-4 and GEOS-5 (Fig. 12). The dynamic impacts at 147 hPa (Fig. 10b) are comparable to the corresponding impact at 147 hPa from the biomass burning emissions. The temporal variations of the biomass burning and the dynamic impacts track closely those at 215 hPa.

Deep convection rarely penetrates the tropical tropopause region (Alcala and Dessler, 2002; Gettelman et al., 2002). As such, both the biomass burning and the dynamic impacts are relatively small (about 15 ppb of CO) at 100 hPa. The biomass burning impacts show notable time lags among the three pressure levels while the dynamic impacts show no obvious time lags. The larger differences of biomass burning impacts between 215 hPa and 147 hPa in GEOS-4 (~100 ppbv CO) than in GEOS-5 (~60 ppbv CO) again reflects the different strengths of deep convection in the respective reanalysis data sets (Figs. 5, 12).

Previous studies showed that during El Niño, both the biomass burning and the changes in meteorological conditions including low convective activity, sparse precipitation, dry air condition, and large-scale dynamical changes contributed to the observed enhancements in tropospheric ozone columns over equatorial Asia (Sudo and Takahashi, 2001; Chandra et al., 2002; Chandra et al., 2009). Our model results show significantly enhanced O_3 concentrations at both 215 hPa and 147 hPa because of the biomass burning emissions (Fig. 11a). For the same reason provided in previous sections, we do not include the model results at 100 hPa in the discussion here. The biomass burning emissions contribute about 5–20 ppbv (GEOS-4) and 10–15 ppbv

ACPD
11, 19357–19393, 2011

(GEOS-5) to the O_3 enhancements in the tropical UT during October and November 2006. The enhancements are larger by about 10 ppb at 215 hPa than those at 147 hPa in the model results driven by GEOS-4 meteorological data but comparable in the model results driven by GEOS-5 meteorological data. These differences reflect the different strengths of deep convection in GEOS-4 and GEOS-5 data. The dynamic impacts on O_3 are complex with O_3 enhancements up to 20–30 ppbv at both 215 hPa and 147 hPa (Fig. 11b). The enhancements at 215 hPa and 147 hPa show similar temporal variations. The dynamic impacts on O_3 show large and frequent fluctuation, which reflects the non-linearity of both the dynamics and the O_3 chemistry.

Lightning NO_x emissions strongly control tropical upper tropospheric O_3 production (Sauvage et al., 2007; and references therein). Logan et al. (2008) suggested that lightning NO_x was a major contributing factor to the positive anomaly in the tropospheric column ozone observed over equatorial Asia by TES during December 2006. Nassar et al. (2009) in a modeling study using GEOS-Chem, showed that lightning NO_x emissions contributed about 5–15 ppb to tropical tropospheric O_3 concentrations over equatorial Asia based on the differences in lightning NO_x between 2005 and 2006 (2006 minus 2005), with the largest contribution in the UT. Lightning and the associated NO_x emissions in the GEOS-Chem model version used here are related to deep convective cloud top height (Sect. 4). Therefore, a large part of the dynamic impact on O_3 shown in Fig. 11b is due to the different lightning activities between 2005 and 2006 as predicted in the model.

6 Summary and conclusions

Observations from the Microwave Limb Sounder (MLS) showed significantly enhanced CO and O_3 levels were observed in the tropical upper troposphere over equatorial Asia during the 2006 Indonesian fires from August to November. We investigated the effect of these fire emissions and dynamics on the tropical upper tropospheric CO and O_3 by interpreting MLS observations using the GEOS-Chem model. The model

ACPD
11, 19357–19393, 2011

captured the seasonal variations and special distributions of CO and O_3 in the tropical upper tropopshere over equatorial Asia. The biomass burning outflow as indicated by CO were primarily driven by tropical easterlies to the Indian Ocean and the western North Pacific subtropical high to the Southeast Asia. GEOS-Chem CO reproduced the distinct time lags between MLS observed CO enhancements at 215, 147, and 100 hPa, reflecting in part the decreasing influence of deep convective lifting with altitude in the tropical upper troposphere. In addition, a time lag of about two weeks between the surface fire emissions and the CO enhancements in the upper troposphere was seen both in the MLS observations and in the model results.. These CO enhancements corresponded with increased cloud ice water content.

The CO and O_3 enhancements in the tropical upper troposphere over equatorial Asia reflected the combined effect of large surface biomass burning emissions from the 2006 Indonesian fires and the dynamic effect during the 2006 El Niño. Biomass burning accounted for about 50–150 ppbv of CO and 5–20 ppbv of O_3 in the tropical upper troposphere below 100 hPa during October and November 2006, with temporal variations driven by biomass burning and deep convection. The dynamic impacts were complex and accounted for up to 100 ppb of CO and 30 ppb of O_3 in the tropical upper troposphere below 100 hPa. The temporal variation of the dynamic impact on CO was driven by deep convection. The variation of the dynamic impact on O_3 depended both on deep convection and the non-linearity of O_3 chemistry.

Acknowledgements. This research was supported in part by NASA grants NNX09AF07G and NNX08AF64G from the ACMAP program. We also acknowledge supports by the NASA Aura Science Team program. The GEOS-Chem model is managed by the Atmospheric Chemistry Modeling group at Harvard University with support from the NASA ACMAP program. Work at Jet Propulsion Laboratory, California Institute of Technology was done under contract with the National Aeronautics and Space Administration.

References

Alcala, C. M. and Dessler, A. E.: Observations of deep convection in the tropics using the Tropical Rainfall Measuring Mission (TRMM) precipitation radar, J. Geophys. Res., 107(D24), 4792, doi:10.1029/2002JD002457, 2002.

Allen, D. J., Rood, R. B., Thompson, A. M., and Hidson, R. D.: Three-dimensional ^{222}Rn calculations using assimilated data and a convective mixing algorithm, J. Geophys. Res., 101, 6871–6881, 1996a.

Allen, D. J., Kasibhatla, P., Thompson, A. M., Rood, R. B., Doddridge, B. G., Pickering, K. E., Hudson, R. D., and Lin, S.-J.: Transport induced interannual variability of carbon monoxide using a chemistry and transport model, J. Geophys. Res., 101, 28655–28670, 1996b.

Benkovitz, C., Scholtz, M., Pacyna, J., Tarrasón, L., Dignon, J., Voldner, E., Spiro, P., Logan, J., and Graedel, T.: Global gridded inventories of anthropogenic emissions of sulfur and nitrogen, J. Geophys. Res., 101(D22), 29239–29253, 1996.

Bey, I., Jacob, D. J., Yantosca, R. M., Logan, J. A., Field, B. D., Fiore, A. M., Li, Q. B., Liu, H. G. Y., Mickley, L. J., and Schultz, M. G.: Global modeling of tropospheric chemistry with assimilated meteorology: Model description and evaluation, J. Geophys. Res., 106, 23073–23096, 2001.

Chandra, S. and Ziemke, J. R.: Tropical tropospheric ozone: Implications for dynamics and biomass burning, J. Geophys. Res., 107(D14), doi:10.1029/2001JD000447, 2002.

Chandra, S., Ziemke, J. R., Tie, X., and Brasseur, G., : Elevated ozone in the troposphere over the Atlantic and Pacific oceans in the Northern Hemisphere, Geophys. Res. Lett., 31, L23102, doi:10.1029/2004GL020821, 2004.

Chandra, S., Ziemke, J. R., Schoeberl, M. R., Froidevaux, L., Read, W. G., Levelt, P. F., and Bhartia, P. K.: Effects of the 2004 El Niño on tropospheric ozone and water vapor, Geophys. Res. Lett., 34, L06802, doi:10.1029/2006GL028779, 2007.

Chandra, S., Ziemke, J. R., Duncan, B. N., Diehl, T. L., Livesey, N. J., and Froidevaux, L.: Effects of the 2006 El Niño on tropospheric ozone and carbon monoxide: implications for dynamics and biomass burning, Atmos. Chem. Phys., 9, 4239–4249, doi:10.5194/acp-9-4239-2009, 2009.

Chen, Y., Li, Q., Randerson, J. T., Lyons, E. A., Kahn, R. A., Nelson, D. L., and Diner, D. J.: The sensitivity of CO and aerosol transport to the temporal and vertical distribution of North American boreal fire emissions. Atmos. Chem. Phys., 9, 6559–6580, doi:10.5194/acp-

ACPD
11, 19357–19393, 2011

9-6559-2009, 2009.
Considine, D. B., Bergmann, D. J., and Liu, H.: Sensitivity of Global Modeling Initiative chemistry and transport model simulations of radon-222 and lead-210 to input meteorological data, Atmos. Chem. Phys., 5, 3389–3406, doi:10.5194/acp-5-3389-2005, 2005.
Doherty, R. M., Stevenson, D. S., Johnson, C. E., Collins, W. J., and Sanderson, M. G.: Tropospheric ozone and El Niño-Southern Oscillation: Influence of atmospheric dynamics, biomass burning emissions, and future climate change, J. Geophys. Res., 111, D19304, doi:10.1029/2005JD006849, 2006.
Duncan, B. N., Martin, R. V., Staudt, A., Yevich, R., and Logan, J. A.: Inter-annual and seasonal variability of biomass burning emissions constrained by satellite observations, J. Geophys. Res., 108(D2), doi:10.1029/2002JD002378, 2003a.
Duncan, B. N., Bey, I., Chin, M., Mickley, L. J., Fairlie, T. D., Martin, R. V., and Matsueda, H.: Indonesian Wildfires of 1997: Impact on Tropospheric Chemistry, J. Geophys. Res., 108(D15), 4458, doi:10.1029/2002JD003195, 2003b
Duncan, B. N., Strahan, S. E., Yoshida, Y., Steenrod, S. D., and Livesey, N.: Model study of the cross-tropopause transport of biomass burning pollution, Atmos. Chem. Phys., 7, 3713–3736, doi:10.5194/acp-7-3713-2007, 2007.
Fu, R., Hu, Y., Wright, J. S., Jiang, J. H., Dickinson, R. E., Chen, M., Filipiak, M., Read, W. G., Waters, J. W., and Wu, D. L.: Short circuit of water vapor and polluted air to the global stratosphere by convective transport over the Tibetan Plateau, Proc. Natl. Acad. Sci., 103, 5664–5669, 2006.
Gettelman, A., Salby, M. L., and Sassi, F.: Distribution and influence of convection in the tropical tropopause region, J. Geophys. Res., 107(D10), doi:10.1029/2001JD001048, 2002.
Guenther, A., Karl, T., Harley, P., Wiedinmyer, C., Palmer, P. I., and Geron, C.: Estimates of global terrestrial isoprene emissions using MEGAN (Model of Emissions of Gases and Aerosols from Nature), Atmos. Chem. Phys., 6, 3181–3210, doi:10.5194/acp-6-3181-2006, 2006.
Hack, J. J.: Parameterization of moist convection in the NCAR community climate model (CCM2), J. Geophys. Res., 99, 5551–5568, doi:10.1029/93JD03478, 1994.
Hudman, R. C., Jacob, D. J., Turquety, S., Leibensperger, E. M., Murray, L. T., Wu, S., Gilliland, A. B., Avery, M., Bertram, T. H., Brune, W., Cohen, R. C., Dibb, J. E., Flocke, F. M., Fried, A., Holloway, J., Neuman, J. A., Orville, R., Perring, A., Ren, X., Sachse, G. W., Singh, H. B., Swanson, A., and Wooldridge, P. J.: Surface and lightning sources of nitrogen oxides

ACPD
11, 19357–19393, 2011

over the United States: Magnitudes, chemical evolution, and outflow, J. Geophys. Res., 112, D12S05, doi:10.1029/2006JD007912, 2007.

Jacob, D. J. and Prather, M. J.: Radon-222 as a test of convection in a general circulation model, Tellus, 42, 118–134, 1990.

Jiang, J. H., Livesey, N. J., Su, H., Neary, L., McConnell, J. C., and Richards, N. A.: Connecting surface emissions, convective uplifting, and long-range transport of carbon monoxide in the upper-troposphere: New observations from the Aura MLS, Geophys. Res. Lett. 34, L18812, doi:10.1029/2007GL030638, 2007.

Jiang, J. H. Su, H., Pawson, S., Liu, H. C., Read, W., Waters, J. W., Santee, M., Wu, D. L., Schwartz, M., Livesey, N., Lambert, A., Fuller, R., and Lee, J. N.: Five-year (2004–2009) Observations of Upper Tropospheric Water Vapor and Cloud Ice from MLS and Comparisons with GEOS-5 analyses, J. Geophys. Res., 115, D15103, doi:10.1029/2009JD013256, 2010.

Jiang, J. H., Su, H., Zhai, C., Massie, S. T., Schoeberl, M. R., Colarco, P. R., Platnick, S., Gu, Y., and Liou, K. N.: Influence of convection and aerosol pollution on ice cloud particle effective radius, Atmos. Chem. Phys. 11, 457–463, doi:10.5194/ acp-11-457-2011, 2011.

Lin, S. J. and Rood, R. B.: Multidimensional flux form semi-Lagrangian transport schemes, Mon. Weather Rev., 124, 2046–2070, 1996.

Liu, H., Jacob, J. D., Bey, I., Yantosca. M. R., Duncan, B. N., and Sachse, G. W.: Transport pathways for Asian pollution outflow over the Pacific: Interannual and seasonal variations, J. Geophys. Res., 108, 8786, doi:10.1029/2002JD003102, 2003.

Liu, J., Logan, J. A., Jones, D. B. A., Livesey, N. J., Megretskaia, I., Carouge, C., and Nedelec, P.: Analysis of CO in the tropical troposphere using Aura satellite data and the GEOS-Chem model: insights into transport characteristics of the GEOS meteorological products, Atmos. Chem. Phys., 10, 12207–12232, doi:10.5194/acp-10-12207-2010, 2010.

Livesey, N. J., Snyder, W. V., Read, W. G., and Wagner, P. A.: Retrieval algorithms for the EOS Microwave Limb Sounder (MLS) instrument, IEEE Trans. Geosci. Remote Sens., 44(5), 1144–1155, 2006.

Livesey N. J., Read, G. W., Froidevaux, L., Lambert, A., Manney, L. G., Pumphrey, C. H., Santee, L. M., Schwartz, J. M., Wang, S., Cofield, E. R., Cuddy, T. D., Fuller A. R., Jarnot, F. R., Jiang, H. J., Knosp, W. B., Stek C. P., Wagner, A. P., and Wu L. D.: Version 3.3 Level 2 data quality and description document, JPL, 2011.

Logan, J. A., Megretskaia, I., Nassar, R., Murray, T. L., Zhang, L., Bowman, W. K., Worden, W. H., and Luo M.: Effects of the 2006 Elo Niño on tropospheric composition as revealed by

data from the Tropospheric Emission Spectrometer (TES), Geophys. Res. Lett., 35, L03816, doi:10.1020/2007GL031698, 2008.
Luo, M., Boxe, C., Jiang, J., Nassar, R., and Livesey, N.: Interpretation of Aura satellite observations of CO and aerosol index related to the December 2006 Australia fires, Atmos. Chem. Phys. Discuss., 9, 23665–23693, doi:10.5194/acpd-9-23665-2009, 2009.
Moorthi, S. and Suarez, M. J.: Relaxed Arakawa–Schubert: A parameterization of moist convection for general circulation models, Mon. Weather Rev., 120, 978–1002, 1992.
Nassar, R., Logan, J. A., Megretskaia, I. A., Murray, L. T., Zhang, L., and Jones, D. B. A.: Analysis of tropospheric ozone, carbon monoxide and water vapor during the 2006 El Niño using TES observations and the GEOS-Chem model, J. Geophys. Res., 114, D17304, doi:10.1029/2009JD011760, 2009.
Olivier, J. G. J. and Berdowski J. J. M.: Global emissions sourcesand sinks, in The Climate System, edited by J. Berdowski, R. Guicherit, and B. J. Heij,, A. A. Balkema, Lisse, The Netherlands, 33–78, 2001.
Ott, L., Duncan, B., Pawson, S., Colarco, P., Chin, M., Randles, C., Diehl, T., and Nielsen, E.: Influence of the 2006 Indonesian biomass burning aerosols on tropical dynamics studied with the GEOS5 AGCM, J. Geophys. Res., 115, D14121, doi:10.1029/2009JD013181, 2010
Randerson, J. T., Liu, H., Flanner, M. G., Chambers, S. D., Jin, Y., Hess, P. G., Pfister, G., Mack, M. C., Treseder, K. K., Welp, L. R., Chapin, F. S., Harden, J. W., Goulden, M. L., Lyons, E., Neff, J. C., Schuur, E. A. G., and Zender, C. S.: The impact of boreal forest fire on climate warming. Science, 314, 1130–1132, 2006.
Rinsland, C. P., Luo, M., Shephard, M. W., Clerbaux, C., Boone, C., Bernath, P. F., Chiou, L., and Coheur, P. F.: Tropospheric emission spectrometer (TES) and Atmospheric Chemistry Experiment (ACE) measurements of tropospheric chemistry in tropical southeast Asia during a moderate El Niño in 2006, J. Quant. Spectrosc. Radiat. Transf., 109, 1931–1942, doi:10.1016/j.jqsrt.2007.12.020, 2008.
Sander S. P., Friedl R. R., DeMore W. B., Golden D. M., Kurylo M. J., Hampson R. F., Huie R. E., Moortgat G. K., Ravishankara A. R., Kolb C. E., and Molina M. J.: Chemical Kinetics and Photochemical Data for Use in Stratospheric Modeling. Technical Report JPL Publication 00-3. Jet Propulsion Laboratory, Pasadena, CA, USA, 2000.
Sauvage, B., Martin, R. V., van Donkelaar, A., Liu, X., Chance, K., Jaegle', L., Palmer, P. I., Wu, S., and Fu, T.-M.: Remote sensed and in situ constraints on processes affecting tropical tropospheric ozone, Atmos. Chem. Phys., 7, 815–838, doi:10.5194/acp-7-815-2007, 2007.

ACPD
11, 19357–19393, 2011

Schoeberl, M. R. and Talabac, S.: The SensorWeb: Afuture technique for science return, in Observing Systems for Atmospheric Composition, edited by: Visconti, G., Carlo, P. D., Brune, W. H., Wahner, A., and Schoeberl, M. R., Springer, New York, USA, 203–206, 2006.
Sudo, K. and Takahashi, M.: Simulation of tropospheric ozone changes during 1997–1998 El Niño: Meteorological impact on tropospheric photochemistry, Geophys. Res. Lett., 28, 4091–4094, 2001.
Thompson, A. M., Witte, J. C., Hudson, R. D., Guo, H., Herman, J. R., and Fujiwara, M.: Tropical tropospheric ozone and biomass burning, Science, 291, 2128–2132, 2001.
Tosca, M. G., Randerson, J. T., Zender, C. S., Flanner, M. G., and Rasch, P. J.: Do biomass burning aerosols intensify drought in equatorial Asia during El Niño, Atmos. Chem. Phys., 10, 3515–3528, doi:10.5194/acp-10-3515-2010, 2010.
van der Werf, G. R., Randerson, J. T., Giglio, L., Collatz, G. J., Kasibhatla, P. S., and Arellano Jr., A. F.: Interannual variability in global biomass burning emissions from 1997 to 2004, Atmos. Chem. Phys., 6, 3423–3441, doi:10.5194/acp-6-3423-2006, 2006.
van der Werf, G. R., Dempewolf, J., Trigg, S. N., Randerson, J. T., Kasibhatla, P. S., Giglio, L., Murdiyarso, D., Peters, W., Morton, D. C., Collatz, G. J., Dolman, A. J., and DeFries, R. S.: Climate regulation of fire emissions and deforestation in equatorial Asia, Proc. Natl. Acad. Sci., 105(51), 20350–20355, doi:10.1073/pnas.0803375105, 2008a.
van der Werf, G. R., Randerson, J. T., Giglio, L., Gobron, N., and Dolman, A. J.: Climate controls on the variability of fires in the tropics and subtropics, Global Biogeochem. Cycles, 22, GB3028, doi:10.1029/2007GB003122, 2008b.
Waters, J. W., Froidevaux, L., Harwood, R. S., Jarnot, R. F., Pickett, H. M., Read, W. G., Siegel, P. H., Cofield, R. E., Filipiak, M. J., Flower, D. A., Holden, J. R., Lau, G. K., Livesey, N. J., Manney, G. L., Pumphrey, H. C., Santee, M. L., Wu, D. L., Cuddy, D. T., Lay, R. R., Loo, M. S., Perun, V. S., Schwartz, M. J., Stek, P. C., Thurstans, R. P., Boyles, M. A., Chandra, K. M., Chavez, M. C., Chen, G. S., Chudasama, B. V., Dodge, R., Fuller, R. A., Girard, M. A., Jiang, J. H., Jiang Y. Knosp, B. W., LaBelle, R. C., Lam, J. C., Lee, K. A., Miller, D., Oswald, J. E., Patel, N. C., Pukala, D. M., Quintero, O., Scaff, D. M., Van Snyder, W., Tope, M. C., Wagner, P. A., and Walch, M. J.: The Earth Observing System Microwave Limb Sounder (EOS MLS) on the Aura satellite, IEEE T. Geosci. Remote, 44(5), 1075–1092, 2006.
Wild, O., Zhu, X., and Prather, M.J.: FAST-J: accurate simulation of in- and below-cloud photolysis in tropospheric chemical models, J. Atmos. Chem., 37, 245–282, 2000
Yevich, R. and Logan J. A.: An assessment of biofuel use and burning of agri-

ACPD
11, 19357–19393, 2011

cultural waste in the developing world, Global Biogeochem. Cycles, 17(4), 1095, doi:10.1029/2002GB001952, 2003.

Yurganov, L. N., McMillan, W. W., Dzhola, A. V., Grechko, E. I., Jones, N. B., and van der Werf, G. R.: Global AIRS and MOPITT CO measurements: Validation, comparison, and links to biomass burning variations and carbon cycle, J. Geophys. Res., 113, D09301, doi:10.1029/2007JD009229, 2008.

Zhang, G. J. and McFarlane, N. A.: Sensitivity of climate simulations to the parameterization of cumulus convection in the Canadian climate centre general circulation model, Atmos. Ocean, 33, 407–446. 10.1029/2005GL022762, 1995.

Zhang, Q., Streets, D. G., Carmichael, G. R., He, K., Huo, H., Kannari, A., Klimont, Z., Park, I., Reddy, S., Fu, J. S., Chen, D., Duan, L., Lei, Y., Wang, L., and Yao, Z.: Asian emissions in 2006 for the NASA INTEX-B mission, Atmos. Chem. Phys., 9, 5131–5153, doi:10.5194/acp-9-5131-2009, 2009.

Ziemke, J. R. and Chandra, S.: Seasonal and interannual variabilities in tropical tropospheric ozone, J. Geophys. Res., 104(D17), 21425–21442, 1999.

Ziemke, J. R. and Chandra, S.: La Niña and El Niño-induced variabilities of ozone in the tropical lower atmosphere during 1970– 2001, Geophys. Res. Lett., 30(3), 1142, doi:10.1029/2002GL016387, 2003.

Ziemke, J. R., Chandra, S., Duncan, B. N., Schoeberl, M. R., Torres, O., Damon, M. R., and Bhartia, P. K.: Recent biomass burning in the tropics and related changes in tropospheric ozone, Geophys. Res. Lett., 36, L15819, doi:10.1029/2009GL039303, 2009

ACPD
11, 19357–19393, 2011

Table 1. Description of model experiments.

Experiment	Year	Meteorological data	Biomass burning emissions
A	2006	GEOS-4	8-day GFEDv2 for 2006
A1	2006	GEOS-4	Monthly climatology
A2	2005	GEOS-4	8-day GFEDv2 for 2006
B	2006	GEOS-5	8-day GFEDv2 for 2006
B1	2006	GEOS-5	Monthly climatology
B2	2005	GEOS-5	8-day GFEDv2 for 2006

ACPD
11, 19357–19393, 2011

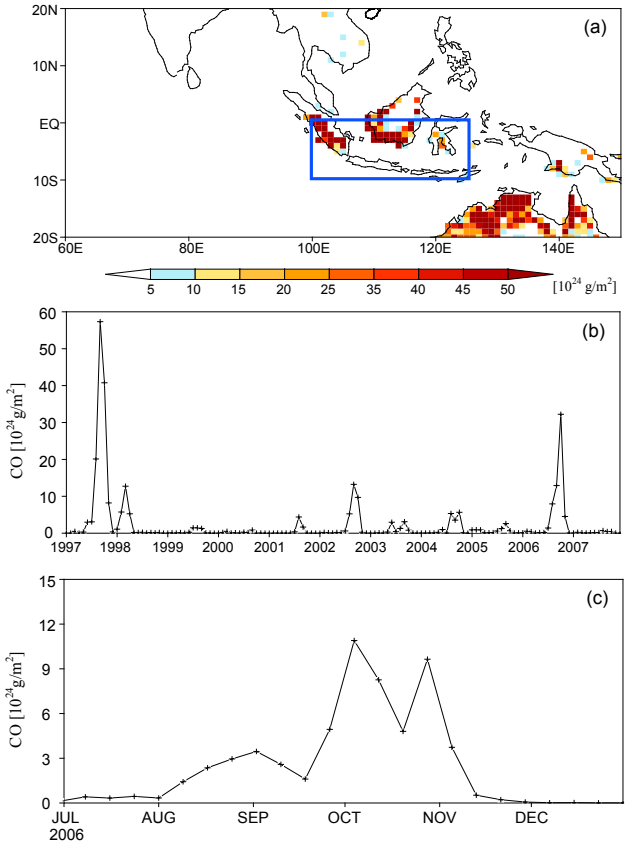

Fig. 1. Carbon monoxide emissions in 2006 over Indonesia and adjacent regions: **(a)** total emissions [10^{24} g/m^2] for August-November 2006, **(b)** monthly emissions over Indonesia (EQ-10° S, 100°–125° E) for 1997–2007, and **(c)** emissions with 8-day temporal resolution over Indonesia from July to December 2006. Data are from the Global Fire Emission Database (GFEDv2) (van der Werf et al., 2006).

ACPD
11, 19357–19393, 2011

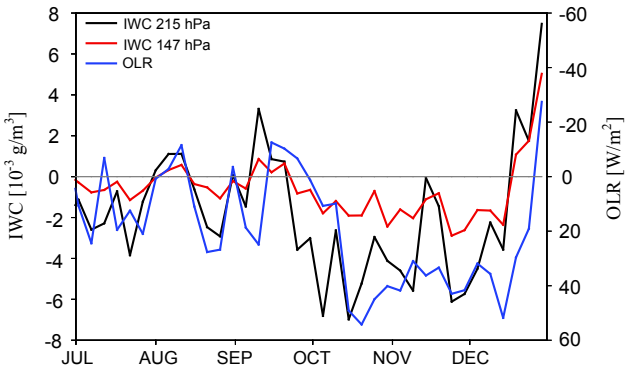

Fig. 2. MLS cloud ice water content (IWC) at 147 hPa and 215 hPa and NCEP/NCAR outgoing longwave radiation (OLR), calculated as the differences between 2006 and 2005. Values are averages over the Indonesia domain (see Fig. 1). Interpolated OLR data provided by the NOAA/OAR/ESRL PSD, Boulder, Colorado, USA, from their website at http://www.esrl.noaa.gov/psd/.

ACPD
11, 19357–19393, 2011

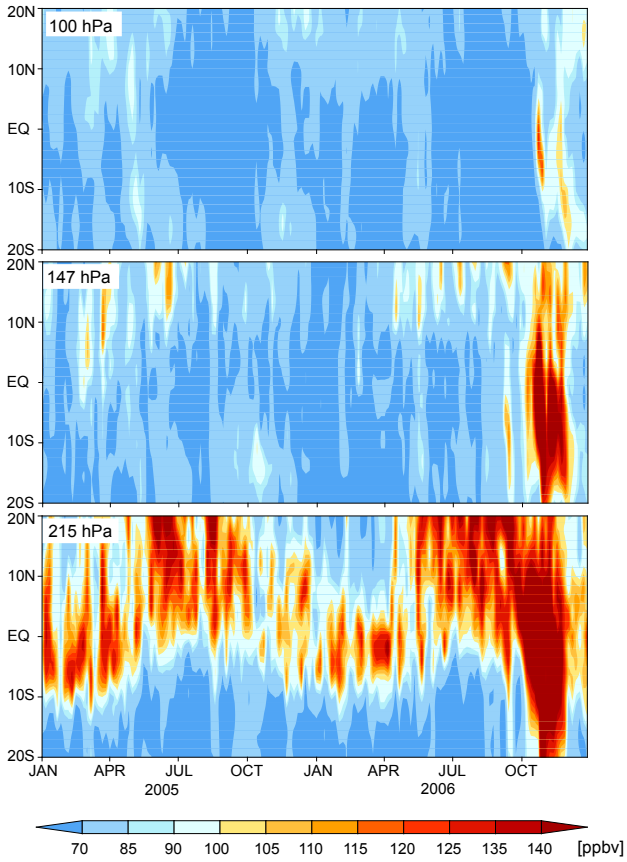

Fig. 3. Time-latitude cross-sections of MLS (v3.3) CO concentrations at 100 hPa, 147 hPa, and 215 hPa from January 2005 to December 2006. Values are averages over 100°–125° E longitudes.

ACPD
11, 19357–19393, 2011

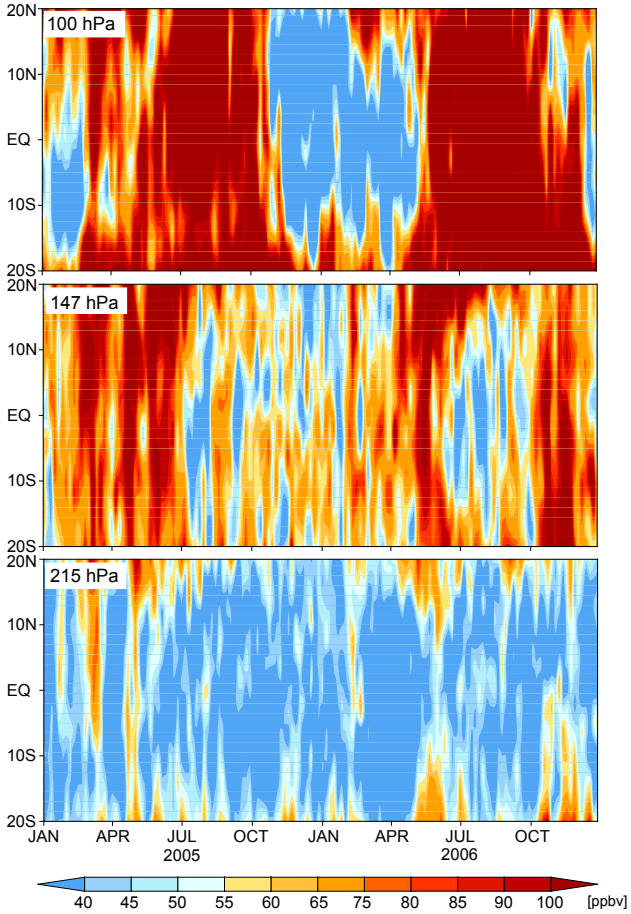

Fig. 4. Same as Fig. 2, but for O_3.

ACPD
11, 19357–19393, 2011

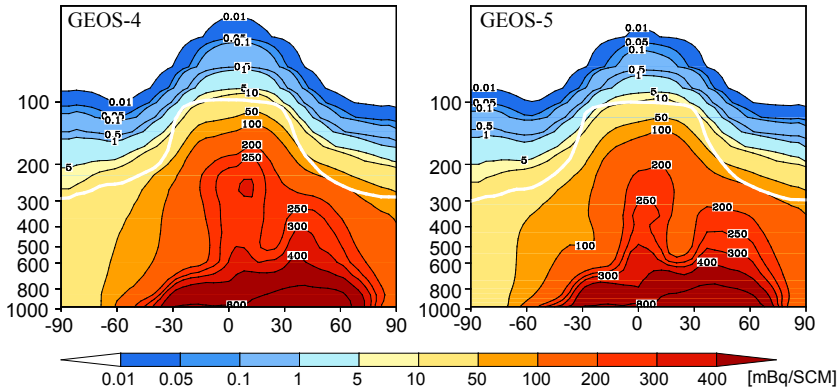

Fig. 5. Annual, zonal mean ^{222}Rn [mBq/SCM] from a GEOS-Chem simulation driven by GEOS-4 and GEOS-5 meteorological data for 2004. White line indicates the World Meteorological Organization (WMO) thermal tropopause.

ACPD
11, 19357–19393, 2011

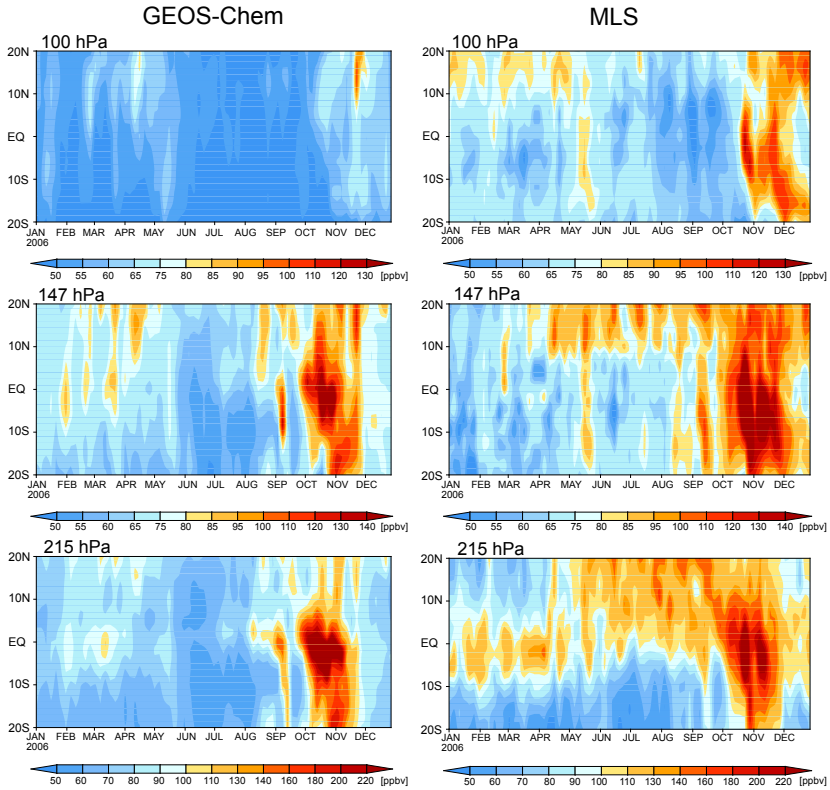

Fig. 6. Time-latitude cross-sections of GEOS-Chem simulated and MLS retrieved CO concentrations at 100 hPa (top panels), 147 hPa (middle panels) and 215 hPa (bottom panels) for 2006. Values are averages over the 100°–125° E longitudes.

ACPD
11, 19357–19393, 2011

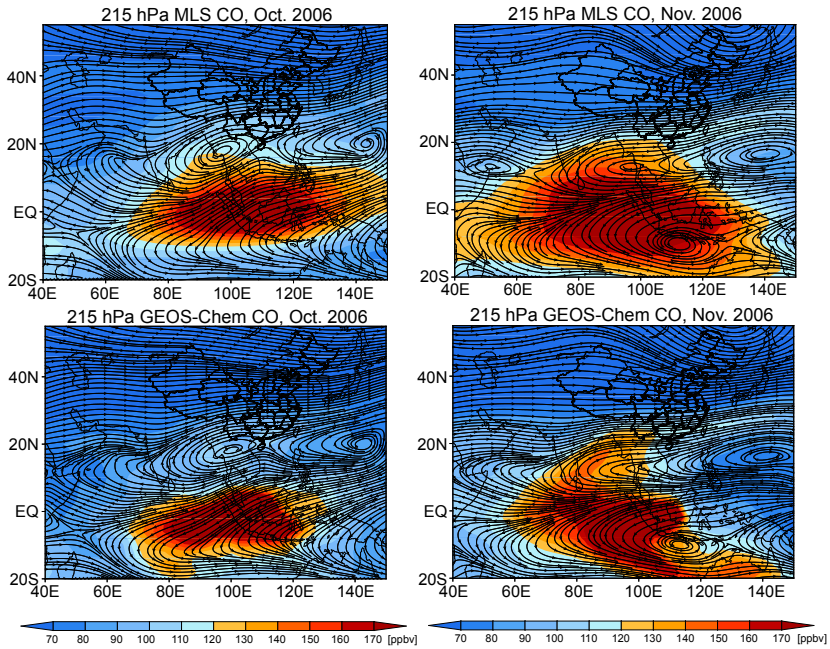

Fig. 7. MLS observed (top panels) and GEOS-Chem simulated (bottom panels) CO concentrations at 215 hPa in October (left panels) and November (right panels) 2006. Also shown are streamlines from NCEP reanalysis data.

ACPD
11, 19357–19393, 2011

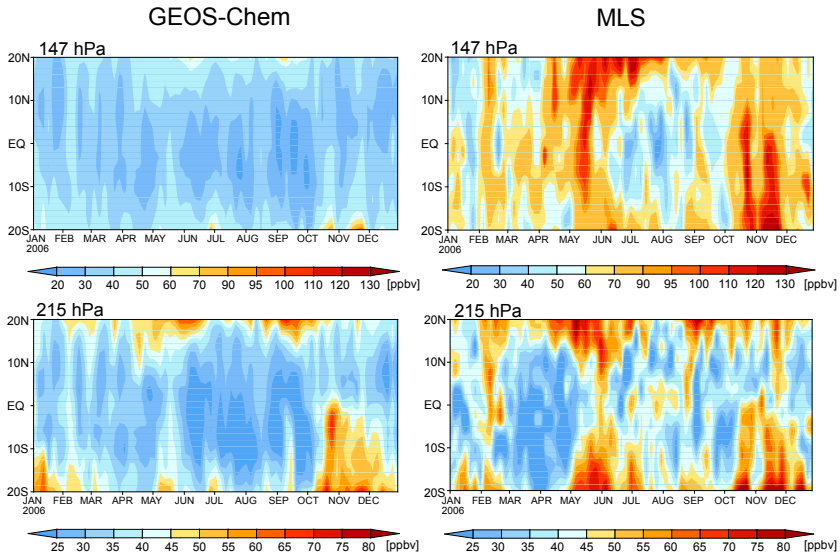

Fig. 8. Same as Fig. 6, but for O_3.

ACPD
11, 19357–19393, 2011

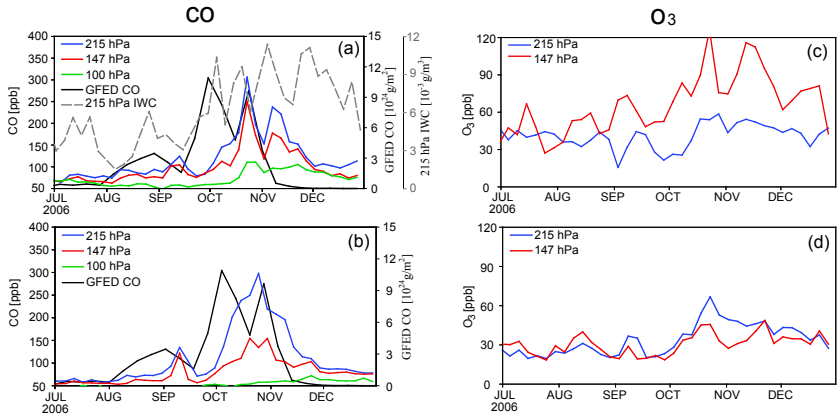

Fig. 9. Upper tropospheric CO and O_3 concentrations over the Indonesia domain (see Fig. 1) from July to December 2006: **(a)** MLS CO at 100 hPa, 147 hPa, and 215 hPa, **(b)** GEOS-Chem simulated CO at 100 hPa, 147 hPa, and 215 hPa, **(c)** MLS O_3 at 147 hPa and 215 hPa, and **(d)** GEOS-Chem simulated O_3 at 147 hPa and 215 hPa. Also shown in **(a)** are 8-day GFEDv2 CO emissions and 215 hPa MLS ice water content (IWC).

ACPD
11, 19357–19393, 2011

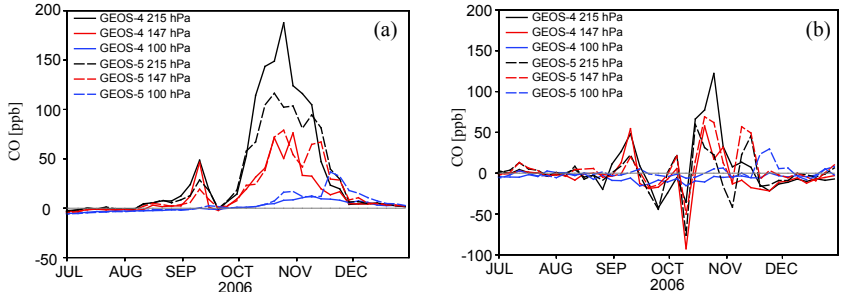

Fig. 10. Simulated upper tropospheric CO concentrations at 100 hPa, 147 hPa, and 215 hPa determined as the differences between two GEOS-Chem simulations: **(a)** both for 2006, but one with GFEDv2 biomass burning emissions for 2006 and the other with climatological biomass burning emissions and **(b)** one for 2006 and the other for 2005 and both with 8-day GFEDv2 biomass burning emissions for 2006. Results from GEOS-Chem simulations driven by GEOS-4 and GEOS-5 meteorological data are both shown. Values are averages over the Indonesia domain (see Fig. 1).

ACPD
11, 19357–19393, 2011

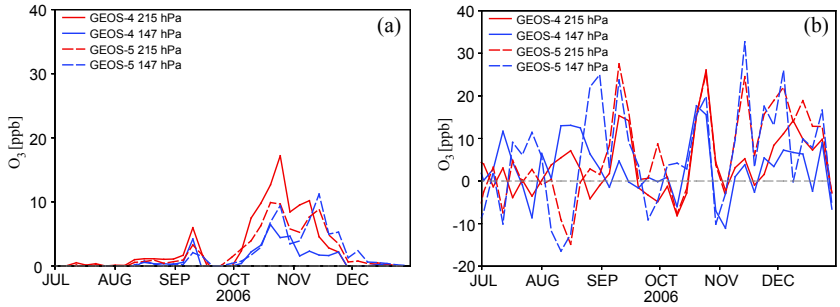

Fig. 11. Same as Fig. 10, but for O_3 at 147 hPa and 215 hPa.

ACPD
11, 19357–19393, 2011

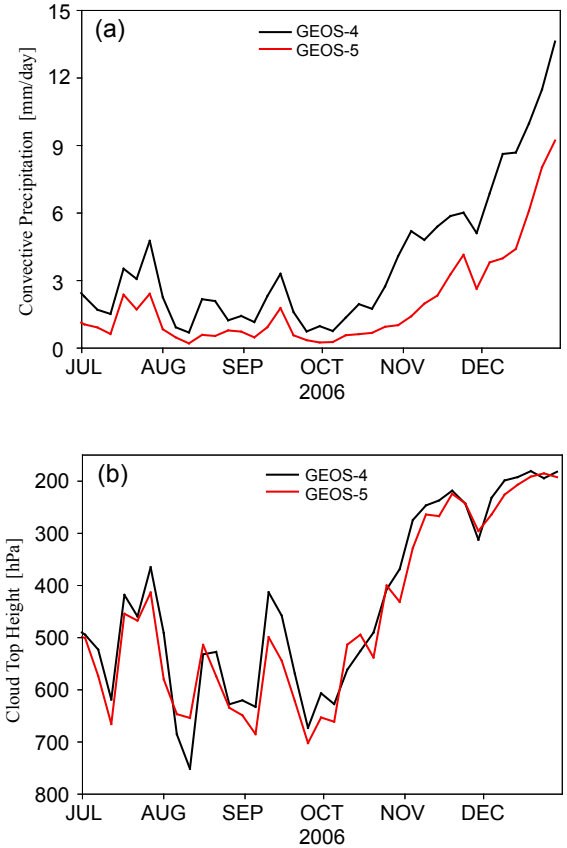

Fig. 12. GEOS-4 and GEOS-5 **(a)** deep convective precipitation rates and **(b)** cloud top height for July–December 2006 over the western and central Indonesian domain (see Fig. 1). Values are 5-day averages.

ACPD
11, 19357–19393, 2011